

MINHA PARK<sup>1</sup>, GANG HO LEE<sup>1,2</sup>, HYO-SEONG KIM<sup>1,2</sup>, BYOUNGKOO KIM<sup>1</sup>,  
SANGHOON NOH<sup>2</sup>, BYUNG JUN KIM<sup>1\*</sup>

## EFFECT OF COOLING RATE ON MICROSTRUCTURE AND MECHANICAL PROPERTIES ACCORDING TO HEAT TREATMENT TEMPERATURE OF INCONEL 625

Inconel 625 is typically used in extreme environments due to excellent mechanical properties such as high strength, corrosion resistance, abrasion resistance and low-temperature toughness. When manufacturing a hot forged flange with a thick and complex shape, the cooling rate varies depending on the location due to the difference in thermal gradient during the cooling process after hot forging. In this study, to evaluate the microstructure and mechanical properties of Inconel 625 according to the cooling rate, we performed heat treatment at 950°C, 1050°C, and 1150°C for 4 hours followed by water cooling. Additionally, temperature data for each location on the flange were obtained using finite element method (FEM) simulation for each heat treatment temperature, revealing a discrepancy in the cooling rate between the surface and the center. Therefore, the correlation between microstructure and mechanical properties according to cooling rate was investigated.

*Keywords:* Inconel 625; Heat treatment; Cooling rate; Microstructure; Mechanical property

### 1. Introduction

Recently, the application of high-performance special materials is increasing for safety and reliability in extreme environments such as high pressure and high corrosion in oil pipeline systems, offshore plants, and crude oil refining facilities. Inconel 625, a Ni-based superalloy, is typically used in extreme environments due to excellent mechanical properties such as high strength, corrosion resistance, abrasion resistance and low-temperature toughness [1-2]. In order to be applied to piping systems in extreme environments, forged flanges manufactured by hot forging are mainly used and have the advantage of obtaining excellent mechanical properties such as high strength and ductility [3-4]. However, when manufacturing a hot forged flange with a thick and complex shape, the cooling rate varies depending on the location due to the difference in thermal gradient during the cooling process after hot forging [5-6]. Therefore, the difference in thermal gradient acts as one of the main factors that generate thermal deformation and thermal stress, resulting in the difference in microstructure and mechanical properties. In order to control the mechanical properties of the forged flange Inconel 625 that are changed by various variables, it is important to investigate the correlation between the microstructure and the mechanical

properties [7-8]. While several studies have recently focused on the mechanical properties of flanges fabricated using nickel-based superalloys, there are a limited number of studies that calculate the cooling rate for each position of the flanges and compare the resulting mechanical properties. Therefore, this study aims to investigate the correlation between microstructure and mechanical properties based on the cooling rate of heat-treated Inconel 625.

### 2. Experimental

The chemical compositions of Inconel 625 used in this study consisted of Ni-20Cr-8Mo-0.15C-0.1Mn-5Fe-0.5Si in wt.%. Inconel 625 was used to make 8 inch diameter weld neck flanges. Inconel 625 flanges are hot forged at 1200°C, followed by a solution heating process in a furnace at temperatures of 950°C, 1050°C and 1150°C for 4 hours followed by water quenching. To determine the cooling rate based on the flange's location, the area was divided into 20 regions, and finite element method (FEM) simulations were used to estimate the cooling rate at each location during water quenching. The cooling rates were classified as fast cooling rate (FCR) and slow cooling rate (SCR) based on the obtained data. The microstructure of Inconel 625

<sup>1</sup> ENERGY SYSTEM GROUP, KOREA INSTITUTE OF INDUSTRIAL TECHNOLOGY, BUSAN 46938, REPUBLIC OF KOREA

<sup>2</sup> PUKYONG NATIONAL UNIVERSITY, DEPARTMENT OF MATERIALS SCIENCE AND ENGINEERING, BUSAN 48513, REPUBLIC OF KOREA

\* Corresponding author: jun7741@kitech.re.kr



was analyzed by optical microscopy (OM) and scanning electron microscopy (SEM). The samples were mechanically grinded with SiC paper and polished with 3, 1, 0.25  $\mu\text{m}$  diamond paste and colloidal silica in final polishing stage. Etching was performed using a 75% hydrochloric acid and 25% nitric acid for 30s-50s. Tensile tests were conducted at room temperature using MTS E45 tensile machine with a capacity of 100 kN and a strain rate of  $10^{-3}/\text{s}$ . The round-type tensile specimens had a gauge length of 24 mm, a width of 6 mm, and a diameter of 2.5 mm. The yield strength was calculated based on the 0.2% offset stress in the specimen, while the elongation was determined by measuring the displacement of the crosshead. Charpy impact tests were carried out at a temperature of  $-46^\circ\text{C}$  using a fully automatic impact test machine with a capacity of 750 J. The geometry of the Charpy impact specimens followed ASTM E23 standards, with dimensions of 10 mm  $\times$  10 mm  $\times$  55 mm and a V-notch with a depth of 2 mm at an angle of 45 degrees. An instrumented impact pendulum device, with a nominal impact velocity of 5.424 m/s, was utilized to obtain the load-displacement curve during the Charpy impact test.

### 3. Results and discussion

Fig. 1 shows schematic illustration of each specimen location according to cooling rate and cooling curve of each specimen obtained by FEM simulation (Forge NxT 3.0, Enginsoft, Rome,

Italy). Metal to metal contact and metal to fluid quenching were applied to the heat transfer simulation. Then, a fast cooling rate (FCR specimen #19) and a slow cooling rate (SCR specimen #9) were selected in two rectangular areas (20 mm  $\times$  19 mm) in Fig. 1(a). They had fast cooling rate (FCR)  $-5.6^\circ\text{C}/\text{s}$ ,  $-6.2^\circ\text{C}/\text{s}$ ,  $-6.8^\circ\text{C}/\text{s}$  and slow cooling rate (SCR)  $-2.4^\circ\text{C}/\text{s}$ ,  $-2.9^\circ\text{C}/\text{s}$  and  $-2.5^\circ\text{C}/\text{s}$  at heat treatment of  $950^\circ\text{C}$ ,  $1050^\circ\text{C}$ ,  $1150^\circ\text{C}$ , respectively in Fig. 1(b).

Fig. 2 shows the microstructure of hot forged Inconel 625 before and after heat treatment according to cooling rate. In the case of the test specimen before heat treatment after hot forging of Inconel 625, a heterogeneous austenite structure in which small grains and coarse grains are mixed was observed, and annealing twins were partially observed in Fig. 2(a and e). In SCR condition, after heat treatment at  $950^\circ\text{C}$ , it was exhibited an austenite structure with inhomogeneous structures with recrystallized fine grains. In 950\_SCR, annealing twins were formed in the irregular and coarse austenite grains with  $150\ \mu\text{m}$  in Fig. 2b. However, the grain size ( $80\ \mu\text{m}$ ) of 950\_FCR (Fig. 2f) was smaller than that of 950\_SCR due to the fast cooling rate. As the temperature increased to  $1150^\circ\text{C}$ , the recrystallized grains were partially formed due to secondary recrystallization [9]. In particular, in SCR specimens, the grain size of austenite structure with homogeneous grains and annealing twins was increased by grain growth in Fig. 2d. However, in the case of FCR specimens (Fig. 2h), an inhomogeneous microstructure was still observed and the grain size was smaller than that of the SCR specimen

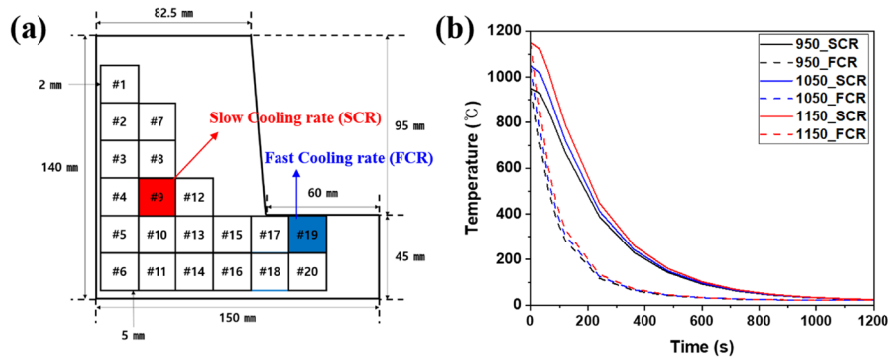


Fig. 1. Schematic illustration of (a) each specimen location according to cooling rate and (b) cooling curve of each specimen obtained by FEM simulation

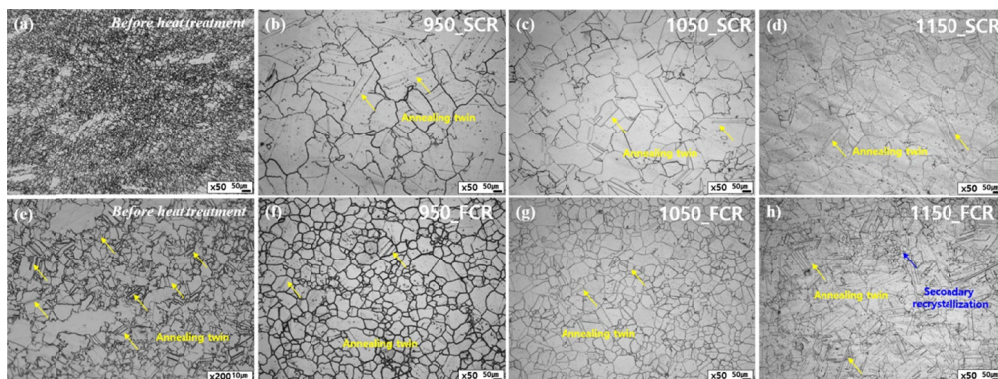


Fig. 2. Optical micrographs of hot forged Inconel 625 before and after heat treatment according to cooling rate: (a and e) before heat treatment after hot forging, after heat treatment (b)  $950^\circ\text{C}$ \_SCR, (c)  $1050^\circ\text{C}$ \_SCR, (d)  $1150^\circ\text{C}$ \_SCR, (f)  $950^\circ\text{C}$ \_FCR, (g)  $1050^\circ\text{C}$ \_FCR and (h)  $1150^\circ\text{C}$ \_FCR

owing to secondary recrystallization. Therefore, microstructure such as grain size and annealing twins were affected according to the heat treatment temperature and cooling rate.

Fig. 3 shows the mechanical properties of hot forged Inconel 625 after heat treatment according cooling rate. Fig. 3a shows the result of tensile properties for hot forged Inconel 625 after heat treatment. With an increase in the heat treatment temperature from 950°C to 1150°C, both the yield strength (YS) and tensile strength (TS) decreased, while elongation increased. This decrease in strength and increase in elongation can be attributed to grain growth and the presence of annealing twins resulting from the elevated heat treatment temperature. Notably, the YS and TS of the specimens subjected to a faster cooling rate (FCR) were

higher compared to those of the specimens with a slower cooling rate (SCR). However, the elongation of the FCR specimens was greater than that of the SCR specimens. Fig. 3b shows the result of hardness properties for hot forged Inconel 625 after heat treatment. At a heat treatment temperature of 1050°C, the hardness exhibited a tendency to be higher, and the FCR specimens had higher hardness values compared to the SCR specimens. This indicates that the FCR specimens, which experienced a relatively faster cooling rate, displayed higher hardness due to the presence of fine grains and an increased number of annealing twins.

Fig. 4(a) shows the results of the absorbed energy and Load-displacement curves obtained by the instrumented Charpy impact test at -46°C according to cooling rate. After heat treatment, the

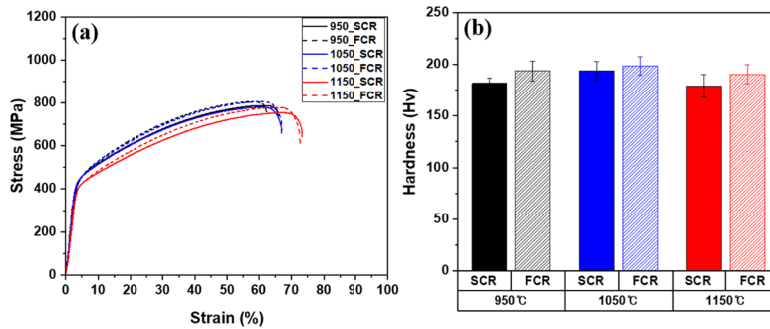


Fig. 3. Mechanical properties of Inconel625 according to heat treatment and cooling rate: (a) stress-strain curves and (b) Hardness property

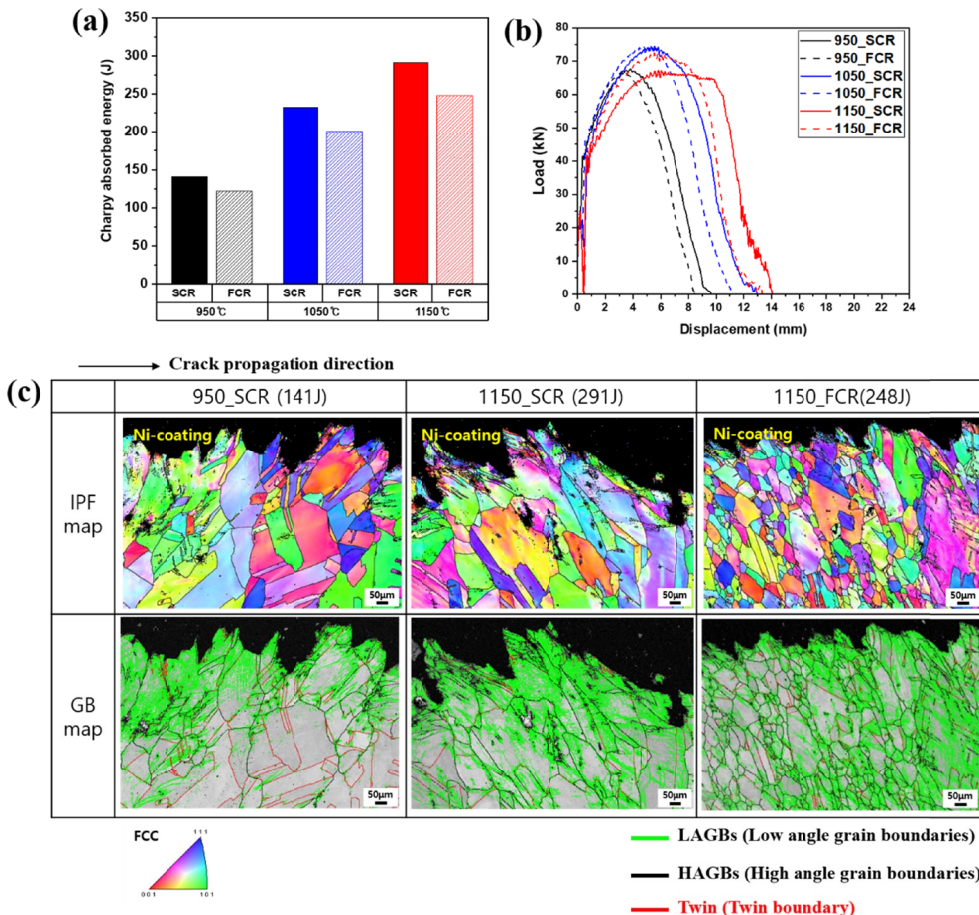


Fig. 4. Charpy impact properties of hot forged Inconel 625: (a) Charpy absorbed energy, (b) Load-displacement curves and (c) Microstructure of the cross-sectional area of the fractured Charpy impact specimens at -46°C



absorbed energy increased as the heat treatment temperature rose from 950°C to 1150°C. When comparing the absorbed energy results according to cooling rate, the specimens subjected to a slow cooling rate (SCR) exhibited higher absorbed energy compared to those with a fast cooling rate (FCR). Furthermore, in comparison to the heat treated specimen at 950°C, the absorbed energy of the specimens treated at 1150°C increased by approximately two times.

Fig. 4b shows the load-displacement curves obtained by the instrumented Charpy impact test at low temperature (−46°C). The crack initiation energy ( $E_i$ ) and crack propagation energy ( $E_p$ ) were calculated by determining the areas below the load-displacement curves based on the maximum load ( $P_{max}$ ) value. The  $P_{max}$  value of the 950\_SCR specimen was approximately 68.4 kN, which exceeded the value of 67.9 kN for the 950\_FCR specimen. Additionally, the crack initiation energy ( $E_i$ ) for the 950\_SCR specimen was around 66 J (47%), whereas for the 950\_FCR specimen, it was approximately 53 J (43%). With an increase in the heat treatment temperature, both the absorbed energy and the ratio of crack initiation energy showed an upward trend. Consequently, the 1150°C heat-treated specimen exhibited significant resistance to crack propagation, indicated by the blunting of the crack at the notch tip.

Fig. 4c shows the microstructure of the cross-sectional area of the fractured Charpy impact specimens at −46°C according to cooling rate. In the 950\_SCR specimen, coarse grains exhibited a small number of low-angle grain boundaries (LAGBs) and numerous annealing twins, allowing for easy propagation of the main crack. In contrast, the 1150\_SCR specimen showed higher crack resistance along the coarse grains during plastic deformation, contributing to the highest absorbed energy [10]. Furthermore, in the 1150\_FCR specimen, the main crack deflected along the fine grains, with a relatively lower presence of LAGBs. As a result, with an increase in heat treatment temperature and a decrease in cooling rate, the absorbed energy increases due to the greater amount of LAGBs within the grain.

#### 4. Conclusions

In this research, we investigated the relationship between the microstructure and mechanical properties of heat-treated Inconel 625, specifically focusing on the influence of cooling rate. The microstructure of the material, including grain size and annealing twins, was found to be affected by both the heat treatment temperature and the cooling rate. We observed that lower cooling rates led to decreased strength and hardness, but increased elongation and absorbed energy. Consequently, as the heat treatment temperature increased and the cooling rate

decreased, the material exhibited improved crack resistance and increased absorbed energy, primarily attributed to the increased presence of low-angle grain boundaries (LAGBs) within the grains.

#### Acknowledgments

This study was supported by the R&D Program of the “Materials/Parts Technology Development Program” (20024858, Development of high manganese steel valves, flange, fitting parts for 40,000 m<sup>3</sup>-class liquid hydrogen transport system).

#### REFERENCES

- [1] C. Dayong, X. liangyin, L. Wenchang, S. Guidong, Y. Mei., *Mat. & Des.* **30** (3), 921-925 (2009).
- [2] H.S. Jeong, J.W. Jeon, M.Y. Ha, J.R. Cho, Finite Analysis for Inconel 625 Fine Tube Bending to predict Deformation Characteristics. *Int. J. Precis. Eng. Manuf.* **13** (8), 1395-1401 (2012).
- [3] M. Kang, M. Park, B. Kim, H.C. Kim, J.B. Jeon, H. Kim, C.Y. Choi, H.S. Park, S.H. Kwon, B.J. Kim, Effect of Heat Treatment on Microstructure and Mechanical Properties of High-Strength Steel for in Hot Forging Products. *Metals* **11** (5), 768-783 (2021).
- [4] B. Rivolta, R. Gerosa, F. Tavasci, L. Ori Belometti, Mechanical and Microstructural Characterization of Forged Inconel 625 Ring Gaskets for Oil and Gas Application. *Mater. Perform. Charact.* **6** (1), 379-387 (2017).
- [5] H. Jo, M. Kang, G.W. Park, B.J. Kim, C.Y. Choi, H.S. Park, S. Shin, W. Lee, Y.S. Ahn, J.B. J, *Metals* **13** (18), 4186-4201 (2020).
- [6] C. Jun, Y. Lee, B.B. Bae, H.-K. Kim, S.S. Hong, D. Kim, J. Yun, E.Y. Yoon, Analyses of creep Properties of Ni-base superalloy powders as cooling rate after solid solution heat treatment. *J. Powder Mater.* **23** (3), 247-253 (2016).
- [7] A. Gunen, E. Kanca, Microstructure and Mechanical Properties of Borided Inconel 625 Superalloy, *Materia* **22**(2), e11829 (2017).
- [8] D. Li, Q. Guo, S. Guo, H. Peng, Z. Wu, The microstructure evolution and nucleation mechanisms of dynamic recrystallization in hot-deformed Inconel 625 superalloy. *Mat. & Des.* **32** (2), 696-705 (2011).
- [9] Y. Wang, Z. Jia, J. Ji, S. Li, D. Liu, Evolution of Stacking Fault and Dislocation during Dynamic Recrystallization of Inconel 625 Alloy. *Adv. Eng. Mater.* **24**, 2200657 (2022).
- [10] J. Rackwitz, Q. Yu, Y. Yang, G. Laplanche, E.P. George, A.M. Minor, R.O. Ritchie, Effects of cryogenic temperature and grain size on fatigue-crack propagation in the medium-entropy CrCoNi alloy. *Act. Mater.* **200**, 351-365 (2020).